Volume 16, Number 3, 2023. pp. 253-259

Jordan Journal of Physics

ARTICLE

Study of Structural and Electronic Properties of TMDC Compounds: A DFT Approach

Vandana B. Parmar and **A. M. Vora**

Department of Physics, University School of Sciences, Gujarat University, Navrangpura, Ahmedabad 380 009, Gujarat, India

Doi: https://doi.org/10.47011/16.3.1

Received on: 10/03/2021; Accepted on: 28/11/2021

Abstract: The structural and electronic properties of transition metal dichalcogenides compounds (TMDC) like TiS_2 and $FeTiS_2$ are studied in the current paper using density functional theory (DFT). The generalized gradient approximation (GGA) with ultra-soft pseudopotential is used under the Quantum ESPRESSO package. From the theoretical data, it is noted the TiS_2 material is a semiconductor in nature with a small indirect band gap. On the other hand, in the doped intercalated compound $FeTiS_2$, which exhibits a metallic nature, the energy bands overlap within the Fermi region. Consequently, $FeTiS_2$ is a ferromagnetic material with spin-up and spin-down characteristics, as also observed from the band structure data.

Keywords: Density Functional Theory (DFT), Generalized Gradient Approximation (GGA), Quantum ESPRESSO code, Intercalated compound.

1. Introduction

Over the past several years, there has been significant interest in studies focused on transition metal dichalcogenides compounds (TMDCs). Layered transition metal dichalcogenides (LTMCDs) have applications in various areas, including lubrication, catalysis, photovoltaics, supercapacitors, and rechargeable battery systems [1]. The dimensionality of a TMDC plays a significant role in its basic physical properties [1]. The study of structural and electronic properties of material gives a basic understanding of the materials [2]. Fang *et al.* have reported *ab initio* band-structure calculations for bulk, single slab, and thin films of TiX_2 (X=S, Se) using the localized spherical wave method [3]. The density functional theory (DFT) based formulation is used for computing the structural and electronic properties of materials [4-7]. The 3d guest atom has been observed to transfer charge from the transition metal Fe-atom to the self-intercalated compound like TiS_2, as reported by Friend and Yoffe [8]. The generalized chemical formula for TMDCs is MX_2, where M represents a group 4 - 6 transition metal and X is a chalcogen element. The TMDCs exist in more than 40 different combinations, each displaying distinct properties.

These materials are deemed attractive for different applications including electronics, photonics, sensing, and energy devices. Unlike graphene, TMDC materials have an intrinsic band gap which makes them suitable for transistor channels reminiscent of an ideal switch for digital logic applications [8]. For example, TiS_2 attracts considerable attention due to the wide range of its potential applications. Specifically, its capacity for engaging with alkali metals, organic molecules, and lithium has positioned it as a valuable asset in the development of lightweight and high-energy-density batteries. Other transition metal

Corresponding Author: A. M. Vora **Email**: voraam@gmail.com

dichalcogenides materials are used as transistors, high-frequency switches, Li-ion batteries, and supercapacitors. Additionally, they have also been considered for use in quantum computer.Generally, in TiS_2, the layer of the Ti atom is sandwiched between two sulphur layers. Both atoms are attracted by very weak van der Waals force and have a very small indirect band gap between them. Because of this, the guest Fe atom can be easily intercalated into a pure TiS_2 compound. Hence, the Fe-S bonds are much stronger than the Ti-S bonds in such $FeTiS_2$ compounds [9]. In both materials, strong hybridization occurs in the 3d-states of Fe, 3d-states of Ti, and 3p-states of S, respectively [10-15]. In electronic property calculations, $FeTiS_2$ exhibits a spin-polarized fully relativistic band structure. The energy bands of TiS_2 do not overlap near the Fermi region, indicating a semi-metallic nature. Conversely, in the case of $FeTiS_2$, these bands overlap near the Fermi region, signifying its metallic nature. This makes these materials suitable for a range of applications, including optoelectronics, high-end electronics, energy storage, and flexible electronics [16-20].

2. Computational Methodology

All the calculations of structural and electronic properties are performed in a DFT environment by using Quantum Espresso code [21] with Burai [22] in our computational laboratory. The structural optimization and the electronic properties such as band structure, density of states (DOS), partial density of states (PDOS), and total density of states (TDOS) of the aforementioned materials are reported using generalized gradient approximation (GGA) [23] with Perdew–Burke–Ernzerhof (PBE) [24] and ultra-soft pseudopotential [25].

3. Results and Discussion

3.1 Structural Optimization

Both the TiS_2 and $FeTiS_2$ compounds have CdI_2-type layer structures, in which the layer of Ti is sandwiched between two layers of sulphur and the unit cell contains four atoms. In the unit cell, the position of Ti is a 1a and those of two S atoms are in 2d (1/3, 1/3, 0.2501) and (2/3, 1/3, -0.2501), respectively. Therefore, the construction consists of an S-Ti-S sandwich-type structure, which is shown in Fig. 1. It is separated by the van der Waals gap along the z-direction [23]. In the presence of very weak van der Waals attraction between the interlayers of Ti and S, guest 3d atoms, such as Fe, can readily intercalate into pure TiS_2. Specifically, the Fe atom occupies a lattice position is 1b (0, 0, 0.5) within the structure. This arrangement forms a hexagonal crystal structure with $P\bar{3}ml$ space group (No. 164) as shown in Fig. 2. In $FeTiS_2$, the lattice parameters are a = 3.4395Å and c = 5.9303 Å. The Brillouin zone (IBZ) for hexagonal crystal structure is shown in Fig. 3.

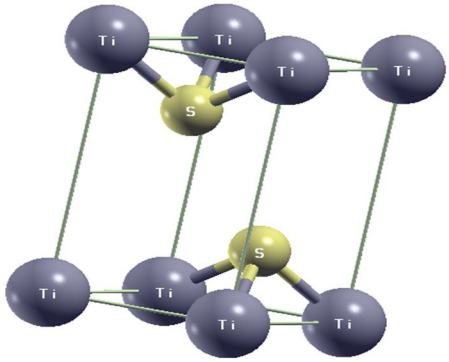

FIG. 1. Crystal structure of TiS_2.

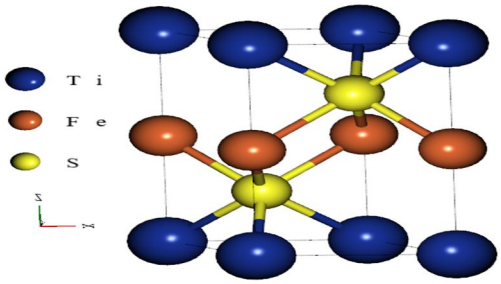

FIG. 2. Crystal structure of $FeTiS_2$.

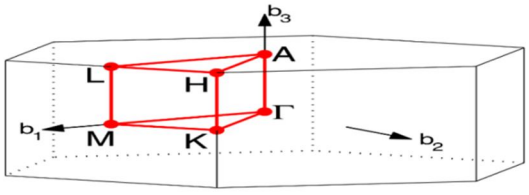

HEX path: Γ-M-K-Γ-A-L-H-A|L-M|K-H

FIG. 3. Brillouin zone for hexagonal structure.

The lattice constant is used to calculate the structural properties of the materials. Here, TiS_2 has a layer with a CdI_2 type structure. The unit cell of this structure includes three atoms. The optimization curves for the ratio of the cell parameters (c/a), kinetic energy cutoff (Ecut), and **k**-grid for TiS_2 and $FeTiS_2$ compounds are shown in Figs. 4 and 5, respectively. Initially,

the lattice constants and the atomic position of all the materials are optimized using the Variable Cell Relaxation (VC-relax) method. After this, the ratio of the lattice parameters (c/a) is optimized for the crystal structure by using the GGA approach with ultrasoft pseudopotential. In Table 1, the computed results of lattice parameters are shown and compared with available theoretical [26] and experimental data [27], which shows qualitative agreement with them. The lattice constants of TiS_2 and $FeTiS_2$ have been calculated and drawn its nature using gnuplot [28] as shown in Fig. 4.

From the calculation for TiS_2 material, the ratio of lattice parameter is 1.7245 Å with Ecut = 60 Ry and **k**-grid = 12×12×12 are taken. For $FeTiS_2$, the respective parameters are 1.6400 Å, 80 Ry, and 16×16×16.

TABLE 1. Calculated lattice parameter of TiS_2 and $FeTiS_2$ compound.

System	Code	Approximation	Lattice Constant (Å)		
			Present	Expt. [27]	Others [26]
TiS_2	QE	GGA	a = 6.4790 c/a = 1.7245	-	-
$FeTiS_2$	QE	GGA	a = 6.4997 c/a = 1.6400	a = 3.3190 c/a = 1.7749	a = 3.4280 c/a = 1.6946

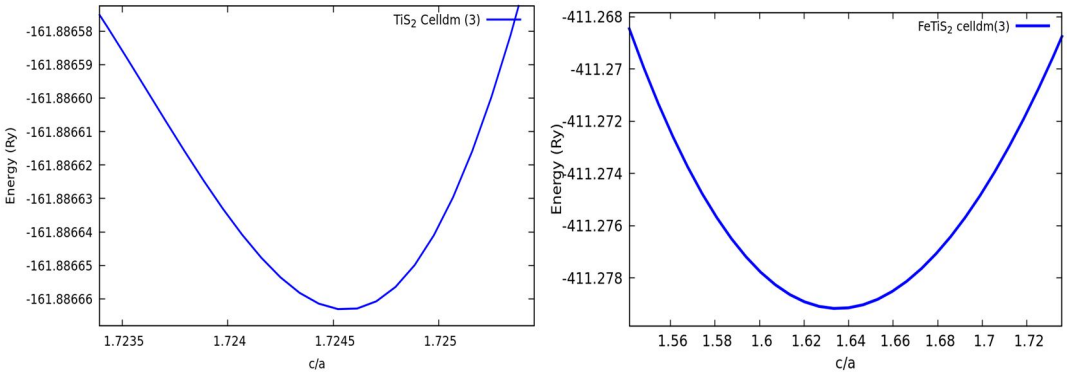

(a) (b)

FIG. 4. Optimization curves for (a) TiS_2 (b) $FeTiS_2$.

3.2 Electronic Properties

In electronic properties, the energy band structure, density of states (DOS), total density of states (TDOS), and partial or projected density of states (PDOS) of the studied are reported.

3.3 Band Structure

The energy band structure of the TiS2 material is shown in Fig. 5, with the **k**-point path plotted on points with high symmetry. This path is of the order of Γ→M→K→ Γ→A. The energy band structures of TiS_2 are displayed in the energy range of -10.0 eV to 10.0 eV. The **k**-path of the band structure includes highly symmetric directions with the irreducible Brillouin zone (IBZ). Generally, the energy band lines are not overlapped near the Fermi region. Hence, the TiS_2 band structure has a semi-metallic material. As shown by previous research, TiS_2 is a semiconductor in nature with a small indirect band gap [13].

The energy band structures of $FeTiS_2$ material are shown in Figs. 6 and 7. Here, the energy band lines are overlapped near the Fermi region. Therefore, the conduction band and valance band are crossed over to each other near the Fermi region in the energy range of -5.0 eV to 5.0 eV. Thus, we conclude that the intercalated compound $FeTiS_2$ has a metallic nature, whereas TiS_2 has a semi-metallic nature. Furthermore, according to the spin-up and spin-down band structures of $FeTiS_2$, the ferromagnetic nature of this compound is observed.

Figure 5 demonstrates that the valance band maxima is overlapped at the Fermi energy level, while the conduction band minima is shown near the Fermi energy level. Therefore, the energy band gap is not observed at Γ→M point in the band structure of TiS_2. TiS_2 is a semi-metallic material [29, 30].

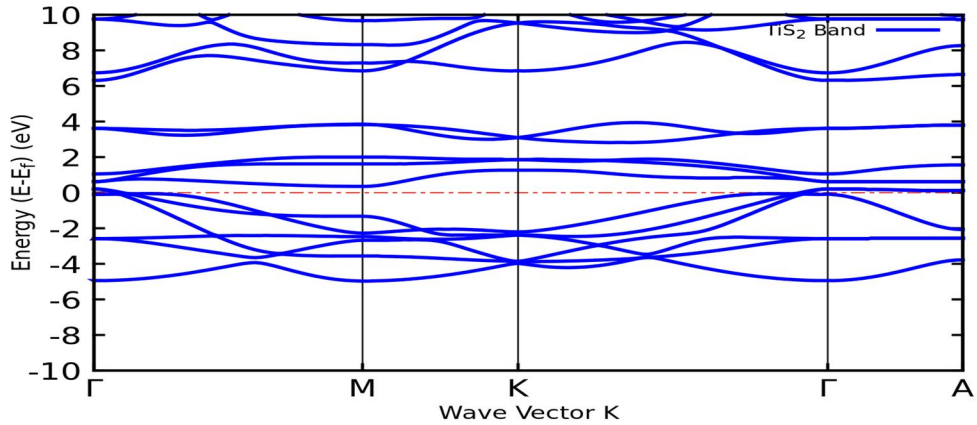

FIG. 5. Electronic band structure of TiS_2.

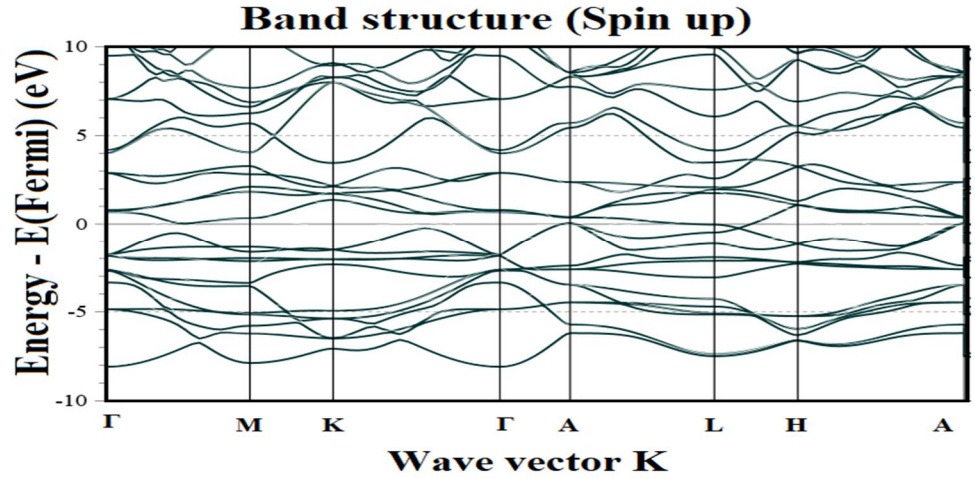

FIG. 6. Electronic band structure of $FeTiS_2$ spin-up.

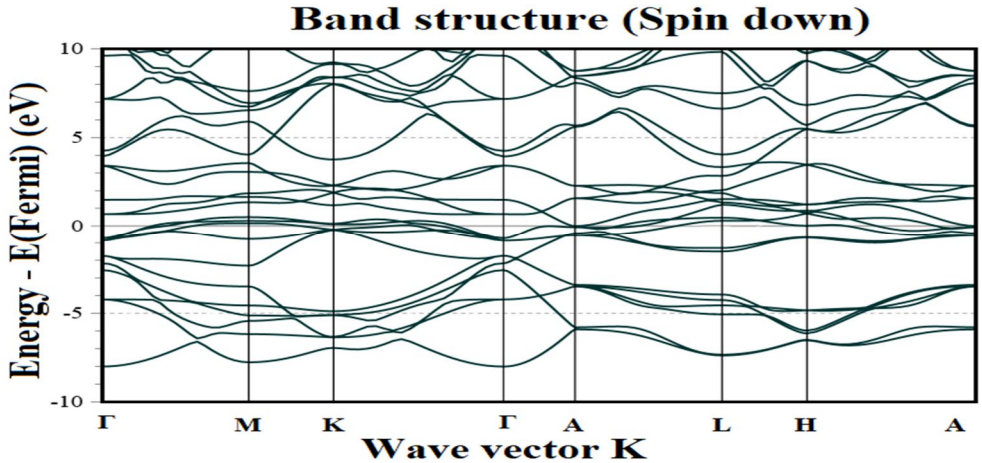

FIG. 7. Electronic band structure of $FeTiS_2$ spin-down.

3.4 Density of States (DOS)

The density of states (DOS) is essentially represented by the number of different states at a particular energy level that electrons are allowed to occupy, the number of electron states per unit volume per unit energy. From the partial or projected DOS, the contributions from the individual orbitals like s, p, d, and f of dissimilar materials are studied [31]. Here, we have applied the tetrahedral method for taking integration over the Brillouin zone to compute the DOS of the materials.

Figures 8 and 9 show the TDOS and PDOS for the TiS_2 compound. It is plotted in the energy range between -10.0 eV to 10.0 eV. In TDOS below the Fermi region, the electron density maximum is at 9.0 states/eV at a point of -3.0 eV. While, above the Fermi region, the electron density maximum at 7.0 states/eV at a point of 2.0 eV, respectively. The DOS at the Fermi

region is shown as a minimum. The 3d-states of Ti and 2p-states of S are drawn in the graph of PDOS of TiS_2. As evident in the PDOS figure, the 3d-states of Ti primarily contribute to the conduction band, while the 2p-states of S mainly contribute to the valance band. Therefore, the TiS_2 shows a semiconductor nature.

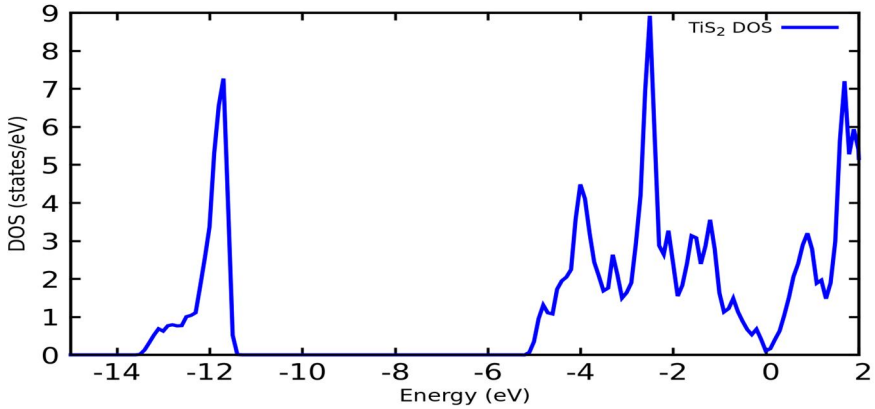

FIG. 8. Total DoS of TiS_2.

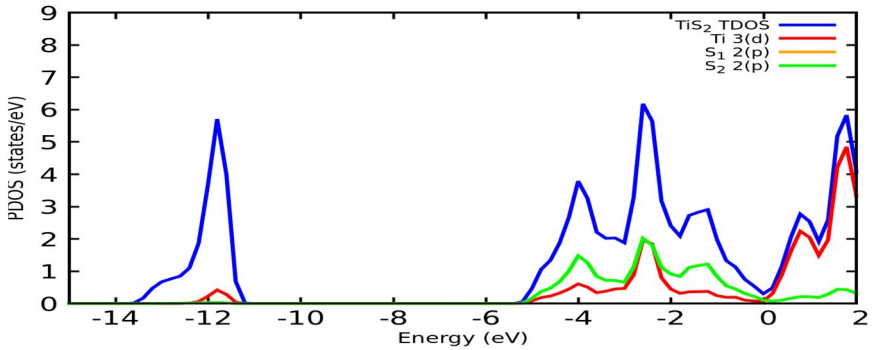

FIG. 9. Partial DOS of TiS_2.

The TDOS and PDOS of $FeTiS_2$ material are shown in Figs. 10 and 11. It is planned in the energy range between -10.0 eV to 10.0 eV in spin-up and spin-down energy states. In TDOS below the Fermi region, the electron density was found maximum at 6.0 states/eV at a point -2.0 eV in spin-up DOS and 3.5 states/eV at a point -4.5 eV in spin-down DOS, respectively. While, above the Fermi region, the electron density maximum was found at 2.0 states/eV at a point 3.5 eV in spin-up and 4.5 states/eV at a point 2.5 eV in spin-down DOS, respectively. The DOS at the Fermi region is shown at 2.5 states/eV. Additionally, in the PDOS of FeTiS2, it is evident that the 3d states of both Fe and Ti make significant contributions to the conduction band, while the 2p states of S primarily contribute to the valance band. This observation underscores the metallic nature of $FeTiS_2$.

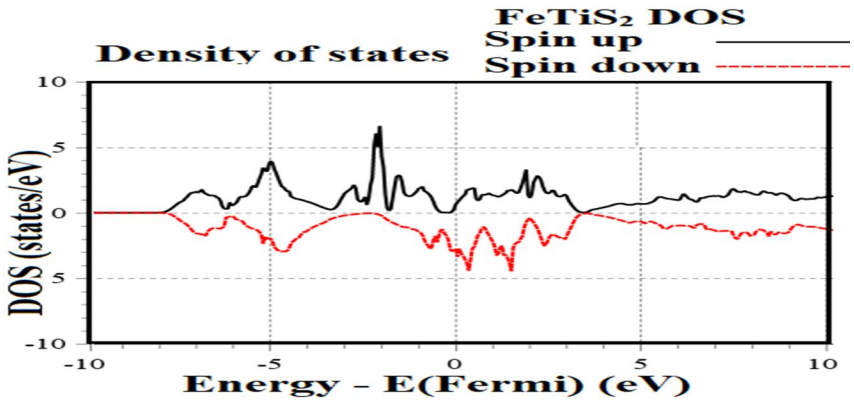

FIG. 10. Total DoS of $FeTiS_2$.

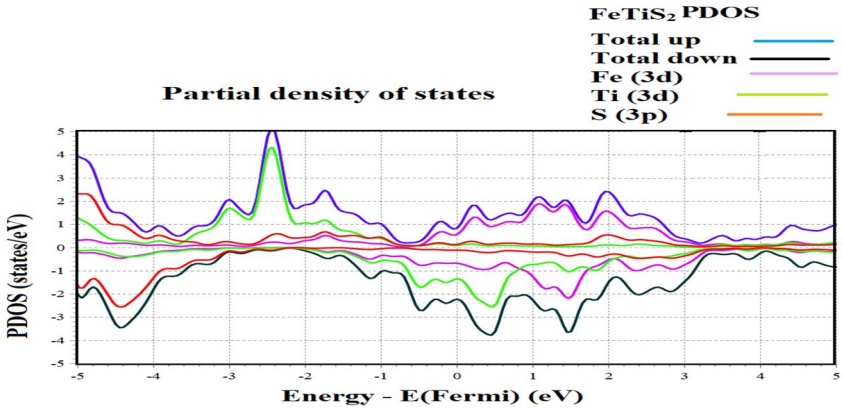

FIG. 11. Partial DOS of $FeTiS_2$.

Guo *et al.*[26] conducted an electron structure analysis of Fe_xTiS_2 compounds using the FP-LAPW method. Their findings indicate that the $FeTiS_2$ compound exhibits a nearly half-metallic ferromagnetic nature with an exceptionally high carrier spin polarization of almost 100% at the Fermi energy E_F. Moreover, they observed substantial splitting in the spin-up and spin-down bands of the Fe-3d components, whereas the bands associated with the Ti-3d or S-3p states do not exhibit significant splitting. These results demonstrate a distinctive nature compared to the data reported previously [26].

4. Conclusions

Our study demonstrates that the structural and electronic properties of intercalated TMDC compounds are successfully carried out using Quantum ESPRESSO code with BURAI software within the DFT framework employing GGA-PBE and ultra-soft pseudopotential. The electronic band structure data clearly reveals the semi-metallic behavior of TiS_2 and the metallic nature of the intercalated compound $FeTiS_2$. From the analysis of the DOS and PDOS, we draw conclusions regarding the contributions of the Fe, Ti, and S atoms to the material and observe their hybridization. Furthermore, by examining the electronic configuration for both spin-up and spin-down states, it becomes evident that FeTiS2 exhibits a ferromagnetic nature.

Acknowledgments

We sincerely acknowledge the computational facility developed under the DST-FIST program from the Department of Science and Technology, Government of India, New Delhi, India, and financial assistance under DRS-SAP-II from the University Grants Commission, New Delhi, India.

References

[1] Zhu, Z.Y., Cheng, Y.C. and Schwingenschlögl, U., Phys. Rev. B, 84 (1) (2011) 153402.

[2] Wang, Q.H., Zadeh, K.K., Kis, A., Coleman, J.N. and Strano, M.S., Nat. Nanotechnologie., 699 (2012) 712.

[3] Fang, C.M., de Groot, R.A. and Hass, C., Phys. Rev. B, 56 (1997) 4455.

[4] Zala, V.B., Vora, A.M. and Gajjar, P.N., AIP Conf. Proc., 2100 (2019) 020027.

[5] Patel, H.S., Dabhi, V.A. and Vora, A.M., In: Singh, D., Das, S. and Materny, A., (Eds.), "Advances in Spectroscopy-molecules to Materials", Springer Proc. Phys., 236 (2019) 389.

[6] Dabhi, V.A., Patel, H.S. and Vora, A.M., AIP Conf. Proc., 2224 (1) (2020) 030003.

[7] Patel, H.S., Dabhi, V.A. and Vora, A.M., AIP Conf. Proc., 2224 (1) (2020) 030006.

[8] Friend, R.H. and Yoffe, A.D., Adv. Phys., 36 (1987) 1.

[9] Wilson, J.A. and Yoffe, A.D., Adv. Phys., 18 (1969) 193.

[10] Suzuki, N., Yamasaki, Y. and Motizuki, K., J. Phys.-Paris Solid State Phys. C, 8 (1998) 49201.

[11] Yamasaki, T., Suzuki, N. and Motizuki, K., J. Phys. C: Solid State Phys., 20 (1987) 395.

[12] Matssushita, T., Suga, S. and Kimuta, A., Phys. Rev. B, 60 (1999) 1678.

[13] Ueda, Y., Negishi, H., Koyana, M. and Inoue, M., Solid State Comm., 57 (1986) 839.

[14] Kim, Y-S., Li, J., Tanaka, I., Koyama, Y. and Adachi, H., Mat. Trans. Jim., 8 (2000) 1088.

[15] Sharma, Y., Shukla, S., Dwivedi, S. and Sharma, R., Adv. Mater. Lett., 6 (4) (2015) 294.

[16] Manzeli, S., Ovchinnikov, D., Pasquier, D., Yazyev, O. and Kis, A., Nat. Rev. Mater., 2 (2017) 17033.

[17] Mak, K. and Shan, J., Nat. Photonics, 10 (2016) 216.

[18] Chhowalla, M., Shin, H., Eda, G., Li, L., Loh, K. and Zhang, H., Nat. Chem., 5 (2013) 263.

[19] Xu, X., Yao, W., Xiao, D. and Heinz, T.F., Nat. Phys., 10 (2014) 343.

[20] Liu, X., Lee, S., Furdyna, J., Luo, T. and Zhang, Y., "Chalcogenide from 3D to 2D and Beyond", (Elsevier, 2020), p. 391.

[21] Giannozzi, P., Baroni, S., Bonini, N., Calandra, M., Car, R., Cavazzoni, C., Ceresoli, D., Chiarotti, G., Cococcioni, M., Dabo, I. and Dal Corso, A., J. Phys. Condens. Matter., 21 (2009) 395502.

[22] http://nisihara.wixsite.com/burai.

[23] Perdew, J.P., Chevary, J., Vosko, S., Jackson, K., Perderson, M., Singh, D. and Fiolhais, C., Phys. Rev. B, 48 (1993) 4978.

[24] Perdew, J.P., Burke, K. and Ernzerhof, M., Phys. Rev. Lett., 77 (1996) 3865.

[25] http://www.quantum-espresso.org/ pseudopotential.

[26] Guo, Y., Yan, H., Gao, G. and Song, Q., Physica B, 405 (2010) 277.

[27] Inoue, M. and Negishi, H., J. Phys. Chem., 90 (1986) 235.

[28] Janert, P., "Gnuplot in Action: Understanding Data with Graphs", (Manning, New York, 2016).

[29] Allan, D., Kelsey, A., Clark, S., Angel, R. and Ackland, G., Phys. Rev. B, 57 (1998) 5106.

[30] Xu, C., Brown, P. and Shuford, K., RSC Advances, 102 (2015) 83876.

[31] Bin, Q., Guo-Hua, Z., Di, L., Jiang-Long, W., Xiao-Ying, Q. and Zhi, Z., Chinese Phys. Lett., 24 (2007) 1050.